20th Australasian Fluid Mechanics Conference
Perth, Australia
5-8 December 2016

Effects of stratification on the dissolution of a vertical ice-face

B. Gayen[1], M. Mondal[1] and R. W. Griffiths[1]

[1]Research School of Earth Science
The Australian National University, Canberra 2601, Australia

Abstract

Numerical simulation is performed to investigate the effect of ambient stratification on a vertical ice face dissolving into cold and saline water. The three coupled interface equations are used, along with the Boussinesq and non-hydrostatic governing equations of motion and equation of state for seawater, to solve for interface temperature, salinity and melt rate. The main focus is on the rate of dissolving of ice at ambient water temperatures between 0° C and 4°C and salinity around 35 psu and the dependence on stratification (as characterizes many sites around Antarctica).

Introduction

The Antarctic and Greenland Ice Sheets have been losing mass at a rapid rate over the past decade. Recent studies suggest that the Antarctic continent lost 310 ± 74 cubic kilometers per year of ice from 2003 to 2012, and that West Antarctic losses are increased by 70% in the past decade [14]. The Pine Island Glacier accelerated 42%, the Smith Glacier accelerated 83%, and the Thwaites Glacier widened and its eastern ice shelf doubled its speed [17, 16, 18]. Antarctic ice-shelves are melting by turbulent transport of heat and salt to the ice face, predominantly under the influence of warmer and salty Circumpolar Deep Water entering ice shelf cavities from the surrounding Southern Ocean [15, 16]. The water exiting ice shelf cavities contributes to Antarctic Bottom Water, providing a crucial component of the global thermohaline circulation. Both heat and salinity play a significant role in the melting process which takes place inside a boundary layer in proximity to the ice-shelf.

The limited availability of field data regarding the thickness and the velocity of the ice, and the position of the grounding line (where the ice shelf meets the ocean floor) make it difficult to determine the mass loss from the Antarctic ice-shelf and the mechanisms responsible. Recent field measurements by Jenkins *et al.* 2010 [9] near Pine Island Glacier used an autonomous underwater vehicle to provide detailed measurements in close proximity to the melting ice sheet. These observations support the idea that the melting and retreat of the ice-shelf grounding line are occurring due to the uptake of heat from relatively warm and salty Antarctic Circumpolar Deep Water [15, 16]. Seawater next to the Antarctic ice shelves is commonly observed to have a stable gradient in salinity and an unstable gradient in temperature [9]. However, the flow field near the ice water interface is very difficult to measure and large uncertainties lie in the accurate prediction of melting rate.

Modelling ice-shelf melting processes is a significant challenge and there are only limited data available from laboratory experiments on melting of ice under oceanic conditions. Groundbreaking experiments [7, 8] showed formation of double-diffusive layers and efficient mixing of melt water from a vertical block of ice in warm water with a salinity gradient. Later, laboratory experiments by Josberger & Martin [10] examined melting of vertical ice-block of O(1)m of height in salt-water of uniform far-field temperature and salinity. Those experiments covered the wide range of surrounding water temperature and characterised the flow near the interface.

Depending on the temperature of the surrounding seawater, ice shelves may either melt or dissolve. Melting will occur when the seawater is sufficiently warm, and it is controlled only by heat transfer [19]. During melting, the interface salinity is zero, and the interface temperature is the melting point of ice (e.g. $0^{\circ}C$ at atmospheric pressure). On the other hand when the sea temperature is close to or below the melting point of fresh ice, dissolution will take place and is governed by a combination of heat and mass transfer [10, 19]. During dissolution, the interface salinity is non-zero, and the interface temperature is less than the melting point of ice and further enhances heat transfer. Recently, laboratory experiments [11] have studied the dissolving process and proposed a theoretical estimation for the scaling of melt rate. In many regions Antarctic seawater stays at temperatures close to $0^{\circ}C$ [17, 15], thus dissolution might play a key role in those environments.

The ice-ocean interaction problem is computationally challenging because the grid size must be sufficiently small that both the thermal (δ_H) and salinity (δ_S) boundary layers are resolved. In particular, δ_S is order of 1 mm, which is an order of magnitude smaller than δ_H [11]. At the micro-level the role of the diffusion of salt to the ice-ocean interface, which leads to dissolution of the ice, is very complex. Most global ocean models [6, 5] and regional ocean modeling systems [2] describe the flow field at a much larger scale ($> O(1)$ km) and rely on parameterizations of the smaller unresolved scales, including the boundary layer against the ice interface. Recently, numerical study covers the dissolution dominated regime using direct numerical simulations by maintaining surrounding water temperature over range of $-1^{\circ}C < T_w < 6^{\circ}C$ [3, 4]. Their results show that melt rate becomes depth independent when boundary layer is turbulent and agree well with the theoretical scaling. It is also noted that the small scale turbulence is maintained by both the buoyancy and the shear production. Many sites around Antarctica seawater are stably stratified with salinity [9] and this may influence the melt dynamics. Here we report the turbulence-resolving simulations to study the melting of ice in the sea-water under the effect of ambient stratifications.

Problem definition

The flow field is solved using direct numerical simulation (DNS) in a three-dimensional tall rectangular domain with length L, height H and width W (in which direction the domain is periodic) shown in figure 1a. The fluid is assumed linear with kinematic viscosity ν, thermal diffusivity κ_T, salinity diffusivity κ_S, coefficient of thermal expansion α and coefficient of haline contraction γ. The flow involves only a small range of temperature over which the real equation of state is usefully approximated as linear without significant effects on the flow. Navier-Stokes equations under the Boussinesq approximation are written in Cartesian coordinates $[x, y, z]$ in dimensional form

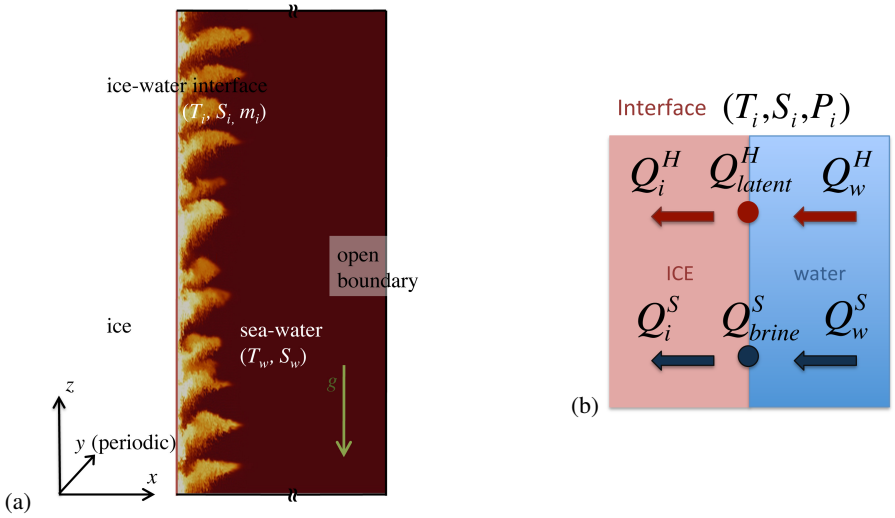

Figure 1: (a) Schematic of the domain used for the simulation: the vertical ice block of height H is placed at the left hand side of the domain and ice-block is contact with sea-water at temperature T_w and salinity S_w. Right hand of the domain has open boundary condition by using a sponge layer. Interface conditions (T_i, S_i and m_i) are evaluated from heat and salinity flux balance at that surface. Superposed is a snapshot of the temperature field $T(C^\circ)$ in the x–z plane from the thermally-equlibrated numerical simulation. (b) Cartoon illustrating heat and salt fluxes.

as:

$$\nabla \cdot \mathbf{u} = 0 \tag{1}$$

$$\frac{D\mathbf{u}}{Dt} = -\frac{1}{\rho_0}\nabla p^* + \nu\nabla^2\mathbf{u} - \frac{\rho^*}{\rho_0}g\mathbf{k} \tag{2}$$

$$\frac{DT^*}{Dt} = \kappa_T\nabla^2 T^* - w\frac{dT^b}{dz} \tag{3}$$

$$\frac{DS^*}{Dt} = \kappa_S\nabla^2 S^* - w\frac{dS^b}{dz} \tag{4}$$

$$\rho^* = \rho_0(\gamma S^* - \alpha T^*) \tag{5}$$

Here, p^*, T^*, S^* and ρ^* denote deviation from the background pressure (p_b), temperature (T_b), salinity (S_b) and density (ρ_b), respectively. The governing parameters are the Grashof number , Prandtl number and Schmidt number,

$$Gr \equiv \frac{\alpha g(T_w - T_i)H^3}{\nu^2} \quad , \quad Pr \equiv \frac{\nu}{\kappa_T} \quad , \quad Sc \equiv \frac{\nu}{\kappa_S}, \tag{6}$$

respectively, where T_i is the interface temperature and T_w is temperature of the surrounding water.

Conservation of heat and salt at the interface ($x = 0$) plays a key role in determining the dissolution velocity [10, 6, 11]. The interface temperature $T_i = a_S S_i$ is controlled by S_i, where the slope of the liquidus is $a_s = -6\times10^{-2}\,^\circ$C/psu and we have neglected the pressure dependent of liquidus over 1m depth scale of the domain. Conservation of heat deals with the balance between latent heat due to dissolution Q_m and the divergence of heat flux ($Q_i^H - Q_w^H$) at the interface as

$$Q_i^H - Q_w^H = Q_m, \tag{7}$$

where $Q_i^H = \rho_s c_s \kappa_T^S \partial T/\partial x$ and $Q_w^H = \rho_w c_w \kappa_T \partial T/\partial x$ are heat fluxes at the interface in the ice and water, respectively and $Q_m = \rho_s L_s V$ is the heat released during ice melting related to the ablation velocity V. Here c_s and κ_T^s is the specific heat and molecular thermal conductivity of ice, where c_w and L_s are the specific heat of the saline water and latent heat of the solid. ρ_s and ρ_w are density of the solid and saline water. To simplify the numerical formulation we ignore the conduction within the ice ($Q_i^H = 0$); the effect of this conductive heat transfer in the dissolution dynamics is described in [11] and is negligible for ice temperatures within several degrees of the interface temperature. The heat balance at the interface is then

$$\rho_s L_s V = -\rho_w c_w \kappa_T \partial T/\partial x. \tag{8}$$

Similarly, a flux balance condition between the fresh water release associated with melting, Q_s (brine rejection), and the salt flux divergence ($Q_i^S - Q_w^S$) at the interface gives

$$Q_i^S - Q_w^S = Q_s. \tag{9}$$

Based on ocean observations [13] the diffusive salinity flux, Q_i^S, in the ice and the salinity in the ice are negligible. The salt balance at the interface is then

$$\rho_s S_i V = -\rho_w \kappa_S \partial S/\partial x. \tag{10}$$

The latter condition maintains the interface salinity at S_i. The ice-water interface is assumed to remain planar and is fixed at $x = 0$. This assumption is based on a large Stefan number ($Sf \gg 1$) and is supported both by a stable, planar interface observed in laboratory experiments [11] and the uniform ablation rate calculated here for the turbulent regime. In any case the assumption is valid over the short duration required for the present solutions. However, we caution that the interface morphology might potentially change with time if there are positive feedbacks between the interface shape, the flow and the ablation rate.

The right hand side boundary of the computational domain is maintained as an open boundary by relaxing temperature and salinity on the boundary back to its background temperature T_b and salinity S_b, respectively. At top and bottom boundaries, no slip condition is imposed for velocities and a no-flux condition is maintained for the temperature and salinity field.

The simulations use a mixed spectral/finite difference algorithm where spanwise (y) derivatives are treated with a pseudo-spectral method, and the wall normal (x and z) spatial derivatives are computed with second-order finite differences. A

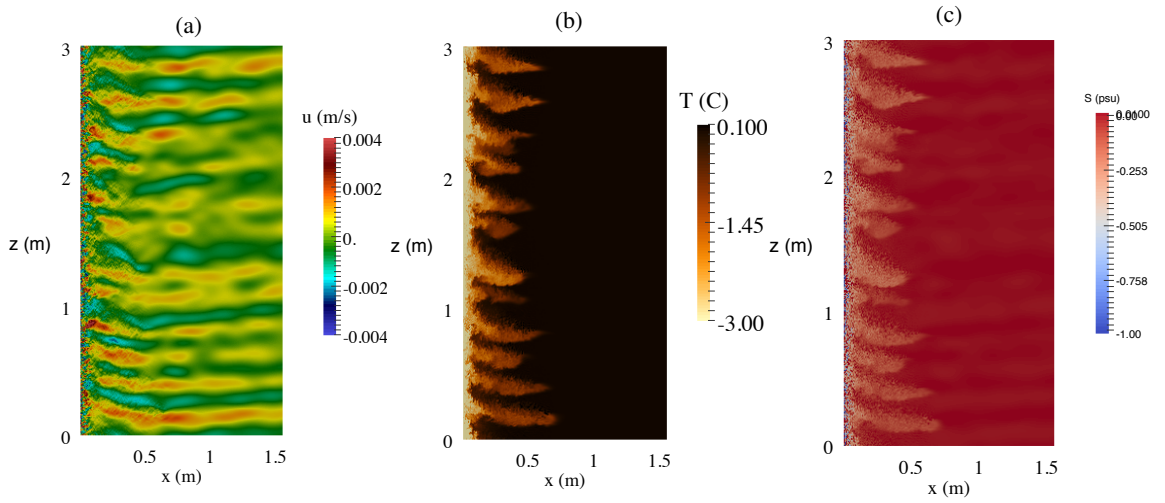

Figure 2: Snapshot of the instantaneous (a) horizontal velocity (u) in x-direction, (b) temperature anomaly and salinity anomaly field on a vertical $x-z$ plane at far field temperature $T_w = 2^\circ C$ and salinity gradient $dS_b/dz = 0.67$ psu m^{-1}.

third-order Runge-Kutta method is used for time-stepping, and viscous terms are treated implicitly with the Crank-Nicolson method. The simulation domain, excluding the sponge region, consists of a rectangular box of $L = 2.5$ m length, $H = 3$ m height and $W = 0.05$ m width. The simulations cover the range $3 \times 10^{10} \leq Gr \leq 2 \times 10^{11}$ with $Pr = 14$ and $Sc = 1500$ (corresponding to a Lewis number $\kappa_T/\kappa_S = 107$). In the simulations, both R_ρ and Sf are large (R_ρ ranges from 20 to 35, while Sf ranges from 10 to 80). The grid size in the test domain is $512 \times 256 \times 1500$ in the x, y and z directions, respectively, with stretching in x and z directions. The grid spacing ($\Delta x_{min} = 0.00001$ m, $\Delta x_{max} = 0.02$ m, $\Delta z = 0.0006$ m, $\Delta y = 0.0004$ m) is sufficient to resolve turbulent micro scales and the salinity boundary layer adjacent to the ice-water interface. Spanwise grid-spacing is determined to be sufficient for DNS by examining the spanwise spectra. Variable time stepping with a fixed Courant-Friedrichs-Lewy number of 1.2 is used which gives time step, $\Delta t \simeq 0.005$ s.

Results

Melting into a stable salinity gradient is examined, where the surrounding water is linearly stratified by salt. Water temperature is kept constant for all the experiments. The flow patten is remarkably different from the uniform ambient case [4]. Here we present a case with far field temperature at $T_w = 2.0^\circ C$, salinity at $S_w = 35$ psu m^{-1} and salinity gradient $dS_b/dz = 0.67$ psu m^{-1}.

In the vicinity of the ice face, the melt water is still buoyant, predominantly due to the fresh water released by melting and moves upwards as a narrow turbulent flow. The external flow which is set up by the temperature difference between far field water (at T_w) and well mixed boundary flow (at T_i), is less influenced by the fresh water exchange from the internal flow, and When this ambient flow approaches the ice-face, it gets cooled by the interior mixed flow and starts sinking. This circulation is shown by horizontal velocity in figure 2a. Because diffusion of salt is much smaller than that of heat, such parcels retain its salinity as they sink in a continuously increasing density field. The height of sinking cannot be more than

$$l_\eta = [\rho(T_w, S_w) - \rho(T_i, S_w)] \Big/ \frac{d\rho_b}{dz}, \qquad (11)$$

where ρ is density as a function of temperature and salinity. The motion creates a series of layers as shown in figure 2. This phenomenon is similar to the previous laboratory observation by [8]. For the present parameters the value of l_η is calculated as $0.3\,m$.The average layer depth is measured to be $0.25\,m$ in our simulation, which is also consistent with layer depths measured in the laboratory [8]. The water travelling away from the ice-face receives heat by double-diffusive convection from warmer and saltier fluid flowing underneath and loses its buoyancy. Internal waves are observed to propagate away from the boundary layer (figure 2a).

Conclusion

Melting into a surrounding salinity gradient forms double-diffusive layers, the thickness of which depends on the ambient density gradient and the difference of density between the freezing point (interface temperature) and the ambient water temperature. Our DNS results successfully reproduce multiple thermohaline layers, as observed in previous laboratory experiments. These layers further affect the shape of the ice-face by making spanwise groves. More quantitative analysis will be performed in future.

Acknowledgements

Computations were carried out using the Australian National Computational Infrastructure, through the National Computational Merit Allocation Scheme supported by the Australian Government. This work was supported by Australian Research Council grant DP120102772. B. G. was supported by ARC DECRA Fellowship DE140100089.

References

[1] Anisimov et al. Section 11.2.1.2: Models of thermal expansion, Table 1.3, in IPCC TAR WG1 2001.

[2] Galton-Fenzi, B. K., Hunter, J. R. , Coleman, R. , Marsland, S. J., Warner, R. C. Modeling the basal melting and marine ice accretion of the Amery Ice Shelf. *J. Geophys. Res.* 2012; **117**, C09031.

[3] Gayen, B., Griffiths, R.W., Kerr, R.C. 2015 Melting driven convection at the ice-seawater interface. IUTAM Symposium on Multiphase flows with phase change: challenges and opportunities, Hyderabad, India, 8-11 December 2014. *Procedia IUTAM*, **15**, 165-171.

[4] Gayen, B., Griffiths, R.W., Kerr, R.C. 2016 Simulation of convection at a vertical ice face dissolving into saline water. *J. Fluid Mech.*, **798**, 284 - 298.

[5] Holland, P. R., Jenkins, A., Holland, D. M. The response of ice shelf basal melting to variations in ocean temperature. *J. Climate.* 2008; **21**: 2558-2572.

[6] Holland D. M., Jenkins A., Modeling thermodynamic ice-ocean interactions at the base of an ice shelf. *J. Phys. Oceanogr.* 1999; **29**:1787-1800.

[7] Huppert H. E., Turner J. S. On melting icebergs. *Nature* 1978; **271**: 46-48.

[8] Huppert H. E., Turner J. S. Ice blocks melting into a salinity gradient. *J. Fluid Mech.* 1980; **100**: 367-384.

[9] Jenkins, A., Dutrieux, P., Jacobs, S. S., McPhail, S. D., Perrett, J. R., Webb, A. T., White, D. Observations beneath Pine Island Glacier in west antarctica and implications for its retreat. *Nature Geosci.* 2010; **3**: 468?472.

[10] Josberger E. G., and Martin S. A laboratory and theoretical study of the boundary layer adjacent to a vertical melting ice wall in salt water. *J. Fluid Mech.* 1981, **111**: 439-473.

[11] Kerr R. C., McConnochie C. D. Dissolution of a vertical solid surface by turbulent compositional convection. *Journal of Fluid Mechanics* 2015; **765** , 211?228.

[12] Morrison, A. K., Hogg, A. McC., Ward, M. L. Sensitivity of the Southern Ocean overturning circulation to surface buoyancy forcing. *Geophys. Res. Lett.* 2011; **38**: L14602.

[13] Oerter H., Kipfstuhl J., Determann J., Miller H., Wagenbach D., Minikin A. Graf W. Evidence for basal marine ice in the Filchner-Ronne ice shelf. *Nature* 1992; **358**: 399-401.

[14] Paolo, F.S., Fricker, H.A. and Padman, L. 2015 Volume loss from Antarctic ice shelves is accelerating. *Science* **348**, 327-331.

[15] Payne, A. J., Vieli, A., Shepherd, A. P., Wingham, D. J., Rignot, E. Recent dramatic thinning of largest West Antarctic ice stream triggered by oceans. *Geophys. Res. Lett.* 2004; **31**, L23401.

[16] Rignot E., Bamber J. L., Van Den Broeke M. R., Davis C., Li Y. H., Van De Berg W. J., Van Meijgaard E. Recent Antarctic ice mass loss from radar interferometry and regional climate modelling.*Nature Geo. Sci.* 2008, **1(2)**: 106-110.

[17] Rignot E., Jacobs, S. S. Rapid bottom melting widespread near Antarctic ice sheet grounding lines. *Science* 2002, **296** 2020-2023.

[18] Rignot, E. et al. 2011 Acceleration of the contribution of the Greenland and Antarctic ice sheets to sea level rise. *Geophys. Res. Lett.* **38**, L05503.

[19] Woods A. W. Melting and dissolving. *J. Fluid Mech.* 1992; **239**:429-448.